



ELSEVIER

Earth and Planetary Science Letters 184 (2000) 251–268

EPSL

www.elsevier.com/locate/epsl

Major element heterogeneity in the mantle source of the North Atlantic igneous province

Jun Korenaga^{a,b,*}, Peter B. Kelemen^b

^a Department of Earth, Atmospheric, and Planetary Sciences, Massachusetts Institute of Technology, Cambridge, MA 02139, USA

^b Department of Geology and Geophysics, Woods Hole Oceanographic Institution, Woods Hole, MA 02543, USA

Received 12 May 2000; received in revised form 13 October 2000; accepted 13 October 2000

Abstract

High-MgO (> 8.5 wt%), aphyric lavas erupted at various locations in the North Atlantic igneous province are utilized to characterize the nature of mantle melting during the formation of this province. Based on the observation that the Ni concentration in residual mantle olivine mostly falls in the range of 2000–3500 ppm, these high-MgO samples are corrected for olivine fractionation until the Ni concentration of equilibrium olivine reaches 3500 ppm, to estimate the composition of primary mantle-derived melt. Estimated primary melt compositions suggest that this province is characterized by significant major element source heterogeneity possibly resulting from basalt addition prior to melting. Primary melts for Southwest Iceland and Theistareykir (North Iceland) are shown to require different source mantle compositions. Whereas the Theistareykir primary melt may be explained by the melting of pyrolitic mantle, the source mantle for Southwest Iceland must be enriched in iron, having molar Mg/(Mg+Fe), or Mg#, < 0.88. This compositional dichotomy in Iceland seems to continue to adjacent Mid-Atlantic Ridge segments, i.e. the Kolbeinsey and Reykjanes Ridges. The primary melts for East and Southeast Greenland also indicate a fertile mantle source, and the estimate of Mg# is the lowest for the East Greenland source mantle (< 0.87). The inferred spatial extent of source heterogeneity suggests the presence of a long-lived compositional anomaly in this igneous province since the opening of the North Atlantic. © 2000 Elsevier Science B.V. All rights reserved.

Keywords: Icelandic plume; hot spots; flood basalts; continental drift

1. Introduction

When Greenland rifted from Europe at about 55 Ma, vigorous magmatism took place along the ~2000-km-long rift, as indicated by the distribution of seaward-dipping reflectors on the North Atlantic margins [1,2]. Within 10 Myr or so, this

spatially extensive voluminous magmatism was reduced in area, but persisted in Iceland (Fig. 1). The impact of an ancestral Iceland plume has been proposed to explain formation of the North Atlantic igneous province in a unified fashion [3,4]. One way to test this hypothesis is to use the composition of lavas to deduce the process of mantle melting and mantle flows. The major element composition of mantle-derived melt is sensitive to pressure and degree of melting as well as style of melting (i.e. batch versus fractional) [5–7]. If one can estimate primary melt com-

* Corresponding author. Tel.: +1-617-253-6299; Fax: +1-617-258-9697; E-mail: korenaga@mit.edu

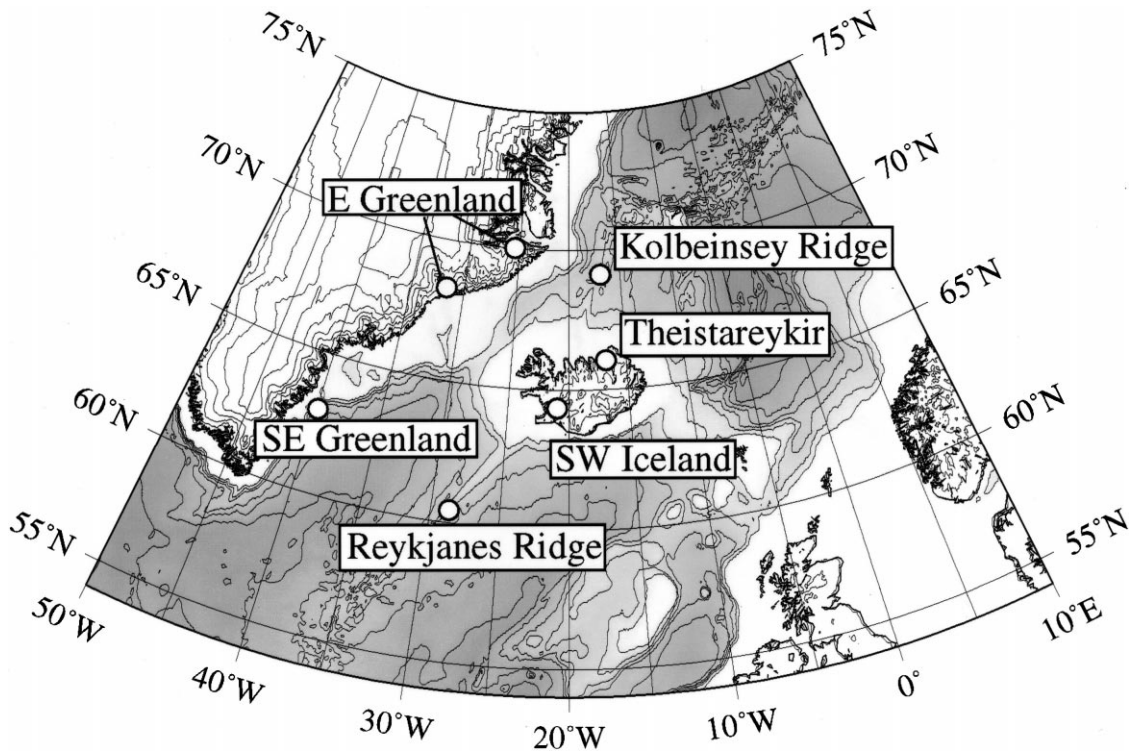


Fig. 1. Map of the North Atlantic showing the locations of six regions considered in this study. Bathymetric contours are at 500-m intervals.

position from observed lavas, then useful constraints on mantle melting may be obtained. Mantle potential temperature can be estimated, and if the thickness of igneous crust is known, the rate of active mantle upwelling can also be calculated. Both types of information are necessary to constrain the thermal state of the mantle and its dynamics.

Erupted lavas have been modified from their primary composition during ascent to the surface. To calculate primary melts, we need to correct for this modification. Fractional crystallization is probably the most important of these processes. At low pressures, fractionating phases from basaltic liquids are generally olivine, then plagioclase, and then clinopyroxene. At higher pressures (>0.5 GPa), clinopyroxene tends to appear earlier than plagioclase (e.g. [8]). It is difficult to accurately correct for multi-phase fractionation, and it is common to apply up-temperature correction only to MgO-rich samples by incrementally add-

ing equilibrium olivine, assuming that olivine was the only fractionating phase. Some criterion has to be adopted to determine how much olivine to add. For example, Fram and Lesher [9], applied an olivine fractionation correction until the liquid Mg# (defined as molar $\text{Mg}/(\text{Mg}+\text{Fe})$) reaches 0.70 or 0.76, using an olivine/liquid $K_D^{\text{Fe}-\text{Mg}}$ of 0.31, assuming that all iron is FeO, and assuming that the forsterite content of residual mantle olivine may vary from 0.88 to 0.91.

Because the Mg# of primary melt depends on melting processes (e.g. the degree of melting) as well as source olivine composition, the Mg# criterion does not serve our purpose of using primary melt composition to infer melting processes. Also, it is impossible to detect heterogeneity in the Mg# of the source. Though major element heterogeneity in source mantle is still poorly understood compared to isotope and trace element heterogeneity, its importance has been suggested for several hotspots including Iceland [10–13]. The

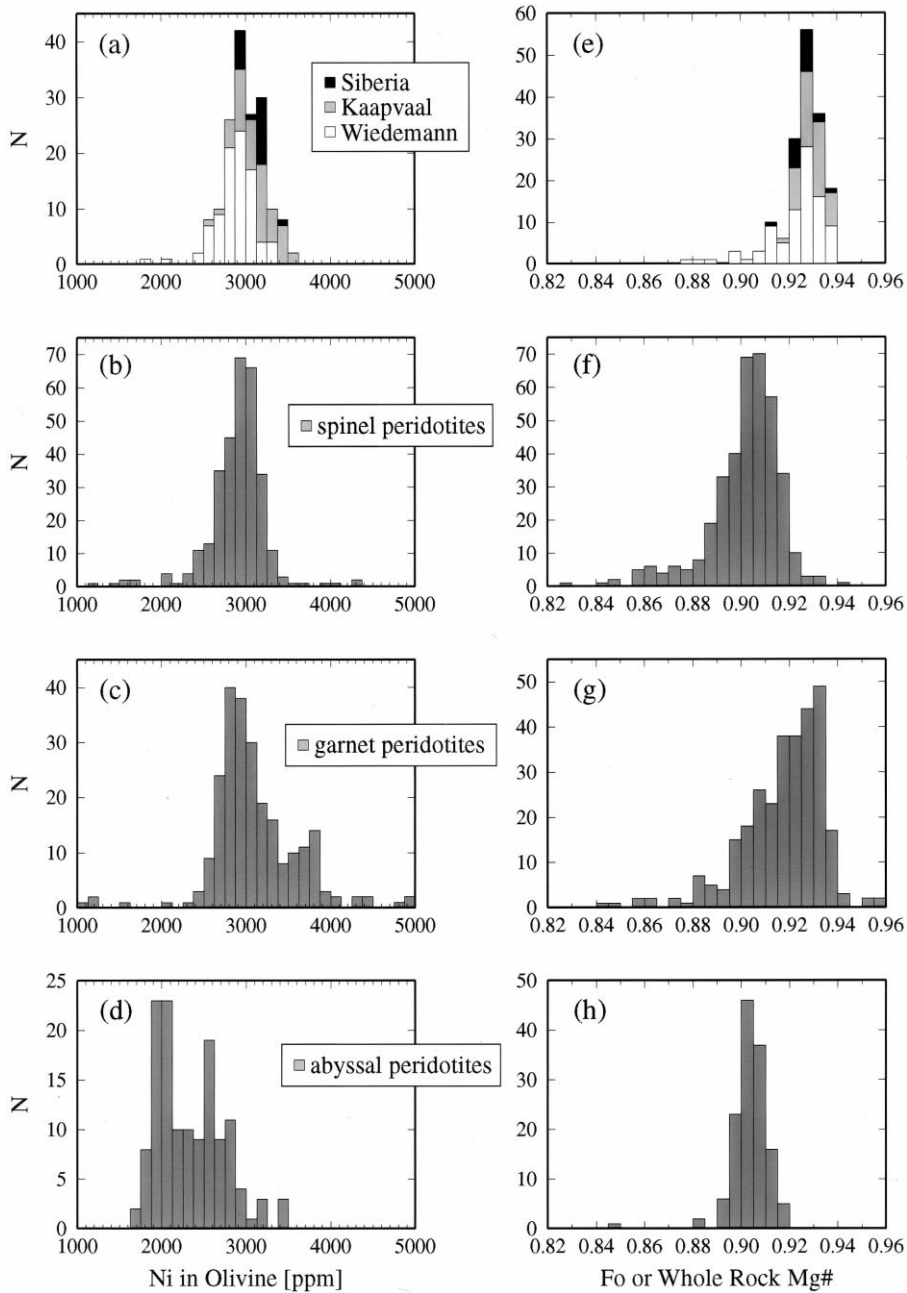


Fig. 2. Histograms of Ni and Fo contents of olivine (or whole rock Mg# for (f) and (g)) in continental and oceanic mantle peridotites. Less than 1% of the data fall outside of the ranges shown. (a) and (e): Mantle xenoliths from East Greenland [55], Siberia [68], and Kaapvaal (F.R. Boyd, personal communication). (b) and (f): Spinel peridotite xenoliths [69], with mineral proportions and Ni contents calculated using from a spinel–herzolite norm [70]. (c) and (g): Garnet peridotite xenoliths [69], with mineral proportions and Ni contents from a garnet–herzolite norm [70]. (d) and (h): Abyssal peridotites (H.J.B. Dick, personal communication).

main process responsible for major element heterogeneity in the mantle is probably the removal (via melting) or addition (via subduction) of a basaltic component [10,14,15]. If this is the case, source olivine composition can serve as a proxy for the degree of heterogeneity. Correcting olivine fractionation based on a fixed composition of residual olivine can mask the signature of major element source heterogeneity that may exist in lava samples.

An alternative criterion that can be used is the Ni content of residual olivine (e.g. [16]). Because Ni is compatible in olivine, its concentration is relatively insensitive to the past history of depletion. The addition of a basaltic component lowers the Ni concentration. A compilation of Ni content in mantle olivine in continental peridotite xenoliths [17] is shown as histograms in Fig. 2. Despite variability in forsterite content, which may be the result of variable depletion, Ni concentration clusters around 3000 ppm, and most of the data are between 2500 and 3500 ppm. The Ni content of olivine in oceanic peridotites shows a similarly tight distribution, but with a lower mean (~ 2500 ppm). Because of the depleted nature of continental peridotites, a value of 3500 ppm can be adopted as an *upper limit* on the likely Ni content of residual mantle olivine, regardless of the degree of major element heterogeneity.

Our procedure for olivine fractionation correction is (1) calculate olivine composition in equilibrium with liquid using an Fe–Mg exchange coefficient, $K_D^{\text{Fe–Mg}}$, and the Ni partition coefficient, $D_{\text{Ni}}^{\text{ol/liq}}$, (2) add 0.1 wt% of the equilibrium olivine to liquid, and (3) repeat (1) and (2) until the Ni content of equilibrium olivine reaches 3500 ppm. $K_D^{\text{Fe–Mg}}$ is nearly constant around 0.30 at low pressures, for a wide range of liquid composition and temperature [18,19], but $D_{\text{Ni}}^{\text{ol/liq}}$ is strongly composition-dependent [20,21]. We use the equation of Kinzler et al. [21], which incorporates all data from previous experimental studies, to calculate $D_{\text{Ni}}^{\text{ol/liq}}$ at each correction step. Our results are virtually unaffected if, instead, we use the equation of Hart and Davis [20]. We note that the temperature dependency of $D_{\text{Ni}}^{\text{ol/liq}}$ is completely incorporated in our method through the dependency of $D_{\text{Mg}}^{\text{ol/liq}}$ on temperature.

The purpose of this paper is to estimate primary, mantle-derived melts, using this olivine fractionation correction, for the North Atlantic igneous province. The estimated melt compositions are discussed in light of recent experimental studies of mantle melting. Our results indicate significant major element heterogeneity in the source of this igneous province. First, we will review the validity of olivine-only fractionation correction for high-MgO samples through modeling of crystallization.

2. Behavior of Ni in crustal modification processes

Modeling of crystal fractionation is conducted at a range of crustal pressures, starting from several sample melt compositions. This exercise helps to identify the type of lavas to which our correction can be safely applied. We use the method of Weaver and Langmuir [22] with extension for high-pressure crystallization by Langmuir et al. [6]. Readers are referred to Yang et al. [23] for a comparison with other models; the difference between predictions of calculated liquid compositions based on the Weaver and Langmuir method and on the Yang et al. method is generally less than a few percent relative. Similarly, both methods agree with experimental data to within 8% relative in terms of mineral compositions. Initial liquids are chosen from experimental partial melts of mantle peridotite compositions, and cover a reasonably wide range of MgO concentration (10–18%; Fig. 3). They are assumed to be in equilibrium with mantle olivine with 3000 ppm Ni. The Ni concentration of liquid is tracked using Kinzler et al. [21] for olivine-liquid partitioning, assuming that $6D_{\text{Ni}}^{\text{cpx/liq}} = D_{\text{Ni}}^{\text{ol/liq}}$ and $D_{\text{Ni}}^{\text{plag/liq}} = 0$ [17,24]. The modeling results are shown in terms of liquid Ni, MgO and the phase proportions of fractionated minerals (Fig. 3). Both fractional and equilibrium crystallization paths are calculated. As Langmuir [25] showed, the liquid line of descent resulting from a periodically replenished magma chamber with constant mass [26] is bounded by these two fractionation paths. Except for the initial liquid with the lowest MgO content, olivine is the first phase to crystallize and, at low

pressure, it is the only fractionating phase until the liquid MgO content drops below 10% (Fig. 3a).

The appearance of plagioclase or clinopyroxene as the second fractionating phase introduces com-

plication in Ni–MgO covariation. Whereas olivine + plagioclase fractionation leads to a continuing decrease in both Ni and MgO concentration (e.g. curve B in Fig. 3a), olivine + clinopyroxene fractionation reduces the decline in Ni content

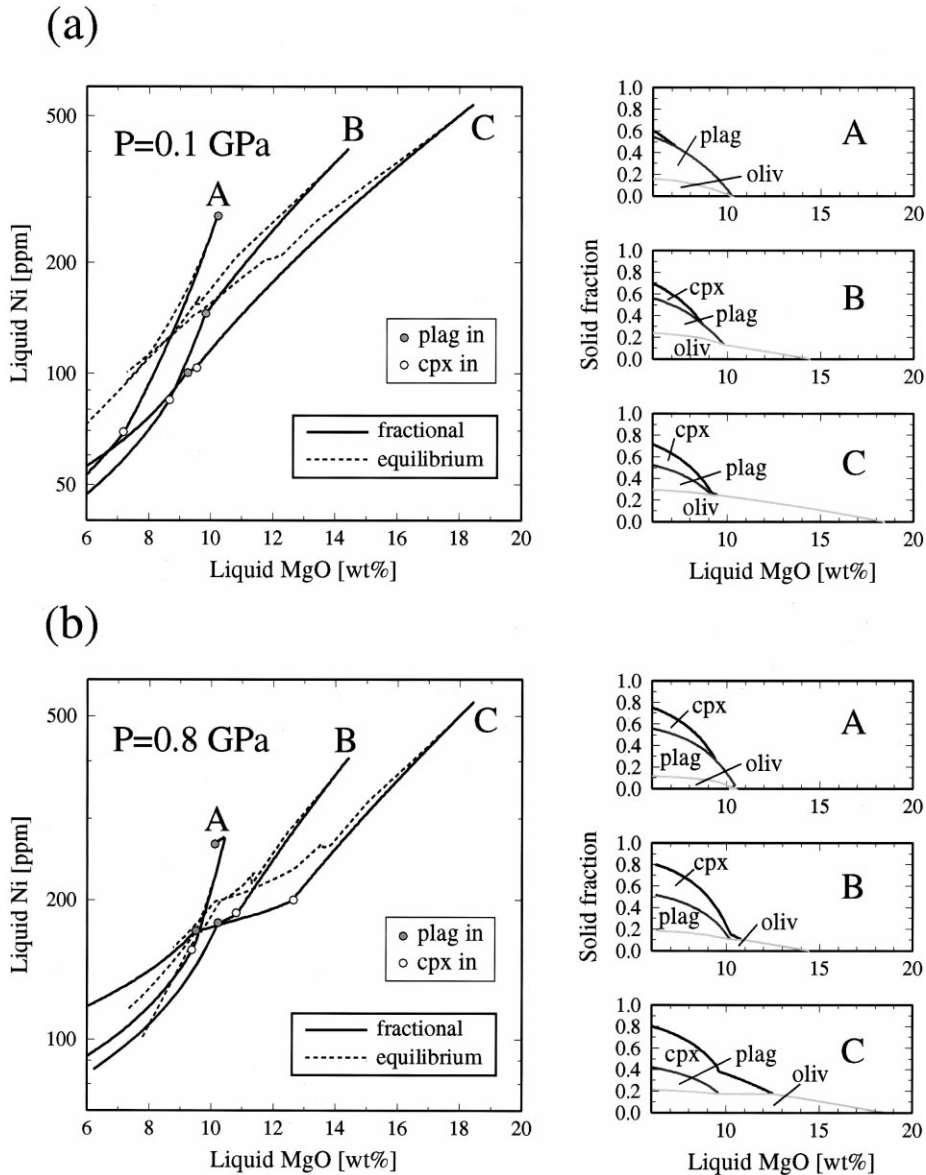


Fig. 3. Results of fractional and equilibrium crystallization modeling are shown in terms of liquid MgO and Ni contents. Temperature decrement was 1°C for fractional crystallization. Cumulative proportion of fractionating phases are also shown for fractional crystallization cases. Starting liquids are A (12% melting of KLB1 at 1 GPa [45]), B (aggregated, near fractional polybaric melts with melt fraction of 11% and mean melting pressure of 1.8 GPa [46]), and C (24% melting of garnet peridotite at 3 GPa [28]). Crystallization pressures are (a) 100 MPa and (b) 800 MPa.

as MgO continues to decrease (e.g. curve C in Fig. 3b). If the olivine-only correction is applied to a liquid on the olivine+plagioclase fractionation path, the MgO content of primary melt tends to be overestimated, and if applied to a liquid on the olivine+clinopyroxene fractionation path, MgO content would be underestimated. Since the MgO content of mantle-derived melt depends on pressure and degree of melting [6,7,27,28], the nature of mantle melting inferred from estimated primary melt composition is sensitive to the validity of the assumption of olivine-only fractionation.

The possibility of plagioclase fractionation may be avoided by using samples with more than 10 wt% MgO. Clinopyroxene can appear above this threshold in high-pressure crystallization (Fig. 3b). However, significant clinopyroxene fractionation without plagioclase would result in a clear change in CaO/Al₂O₃. Such a signal has not been found in lavas with > 10 wt% MgO in our study area (e.g. [9,29,30]). Therefore, we regard the high-pressure liquid line of descent with early clinopyroxene fractionation (e.g. Fig. 3b, liquid C) as a rare case in our study area, and will not consider it further.

Thus, olivine-only fractionation correction for uncontaminated samples with > 10 wt% MgO is a robust procedure to estimate primary melt composition. However, this criterion for sample screening is so strict that the number of available data is too small. By relaxing the MgO threshold to 8.5 wt%, we attempt to obtain the upper bound on the amount of olivine used in correction. Possible plagioclase fractionation would lower the amount of olivine addition required for a given Ni criterion. This upper bound approach conforms to our use of a ‘maximum’ value of 3500 ppm Ni in olivine as the endpoint of fractionation correction. The estimated MgO, therefore, can be regarded as the upper limit on its primary content.

On the other hand, plagioclase fractionation can substantially increase liquid FeO. Ignoring this would lead to an overestimate of FeO content in primary melt. Care must be taken, therefore, to verify that FeO in estimated primary melts is not biased by fractionation correction on low-MgO

samples. To this end, we also apply multiphase fractionation correction, in which 65% plagioclase and 35% olivine assemblage is incrementally added until liquid MgO reaches 10 wt%. The composition of equilibrium plagioclase is calculated based on the method of Weaver and Langmuir [22]. The phase proportions are chosen on the basis of our forward modeling. Though up-temperature correction for multiphase fractionation is fundamentally underdetermined, and our method is not expected to be accurate, we believe that this empirical approach can provide realistic bounds on primary MgO and FeO contents when data are dominated by samples with < 10 wt% MgO.

3. Composition of primary mantle melts for the North Atlantic igneous province

To apply our olivine fractionation correction with the olivine Ni criterion, samples must be aphyric, have MgO > 8.5 wt% and have reported Ni concentration. Though there are numerous studies on the North Atlantic igneous province (e.g. references in [9]), the number of data that satisfy these conditions is limited. The majority of reported lava samples are polyphyric. When a modal analysis is given, we classified samples with less than 5% phenocrysts as ‘nearly-aphyric’, and both aphyric and ‘nearly-aphyric’ samples are used. Six regions have sufficient data for estimation of primary melt composition: Southeast Greenland, East Greenland, Southwest Iceland, Theistareykir (North Iceland), the Reykjanes Ridge and the Kolbeinsey Ridge [9,11,31–35] (Fig. 1).

All data are normalized on an anhydrous basis, and Fe³⁺/ΣFe of 0.05 is assumed [36]. A constant $K_D^{\text{Fe-Mg}}$ of 0.30 is used to calculate equilibrium olivine composition; changing this value by ± 0.01 has only minor influence on our results. In addition to the correction for fractional crystallization, we also calculated correction for equilibrium crystallization of olivine, to explore the extent of ambiguity introduced by a periodically replenished magma chamber. The correction paths for equilibrium crystallization, however,

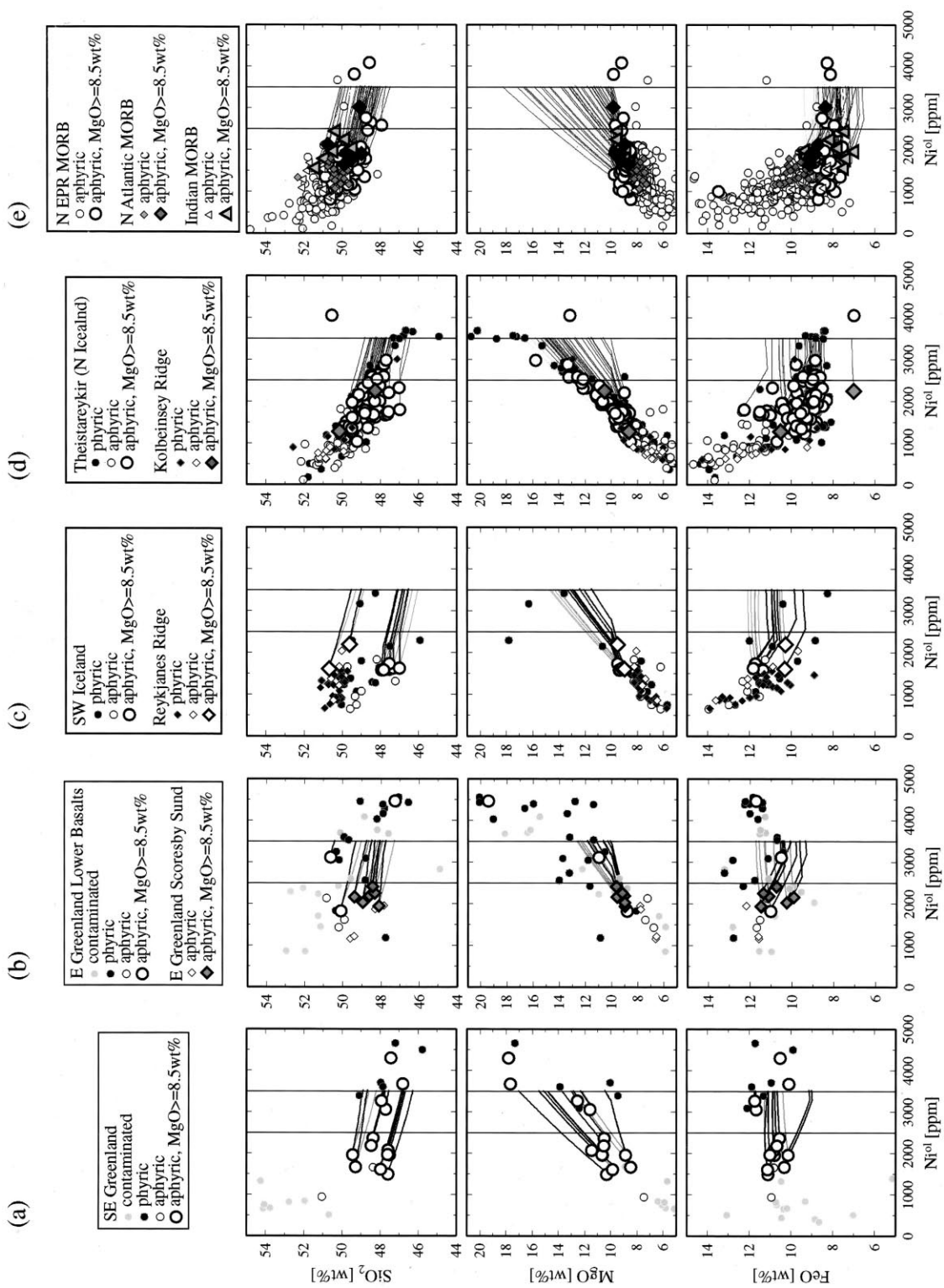


Fig. 4. Results of fractionation correction for lava samples from the North Atlantic igneous province and mid-ocean ridges. Solid curves denote correction for multi-phase fractional crystallization, and dashed curves for olivine-only fractional crystallization. The range of $D_{Ni}^{ol/liq}$ used in these corrections is about 5–10. (a) Southeast Greenland lava samples [33]. (b) East Greenland samples [9]. (c) Southwest Iceland and the Reykjanes Ridge [11,34,35]. (d) North Iceland and the Kolbeinsey Ridge [11,31,34,35] and (e) normal mid-ocean ridges (the northern EPR, the North Atlantic, and the Indian Ocean, data sources in text).

generally deviate from trends shown by North Atlantic lava series [37], and we infer that fractional crystallization is the dominant modification process.

Data for Southeast Greenland are from flood basalt sequences drilled in ODP Leg 152 [33,38]. Following Larsen et al. [33], we screen out samples with $Ba/Zr > 1.5$, which may be contaminated by continental crust. Uncontaminated lavas are mainly in the Upper Series of Hole 917A. There are clearly two magma series in the Upper Series, with different levels of enrichment in TiO_2 and some trace elements [33], but they are similar in terms of other major elements. The results of fractionation correction are shown in Fig. 4a. The estimated upper bounds on primary MgO contents at 3500 ppm Ni in olivine vary from 12.7 to 17.0 wt%, but most are below 15.0 wt%. Olivine addition does not significantly modify FeO, and the mean primary FeO content is 11.0 wt%. SiO_2 as well as other minor elements (e.g. TiO_2 and Na_2O) all decrease as a result of fractionation correction.

Two high-MgO, aphyric lavas have equilibrium olivine with > 3500 ppm Ni (Fig. 3a) prior to fractionation correction. These are not considered in our results. These high-Ni lavas have higher MgO and lower FeO than the average of estimated primary melt compositions, suggesting that they may have resulted from dissolution of cumulative olivine in ‘superheated’ melt. We will discuss possible olivine dissolution in a subsequent section. Interestingly, Thy et al. [30] interpreted these lavas (Units 14 and 16 in their Table 7) as candidates for primary melt, mainly because they are aphyric with high-MgO contents.

Data on East Greenland early Tertiary flood basalts are from Larsen et al. [32] and Fram and Leshner [9], and the results of fractionation correction are shown in Fig. 4b. The data of Larsen et al. [32] are from the Plateau Basalts. We only consider aphyric ‘MORB-type basalts’ and ‘olivine tholeiites’ (L. Larsen, 2000, personal communication). The data of Fram and Leshner [9] are from the Lower Basalts, underlying the main plateau lavas. The identification of uncontaminated lavas follows the approach of Fram and Leshner [9] based on $^{143}Nd/^{144}Nd$, La/Zr and/or Zr/Ti .

Though these data sets may include more than one magma type, their major element compositions are similar, so they are treated collectively to derive a regional estimate for East Greenland.

Olivine in equilibrium with estimated primary melts from East Greenland flood basalts and ODP Leg 152 samples has forsterite from 0.865–0.883, lower than conventionally assumed residual olivine compositions (Fo_{89-91}). Fram and Leshner [9] made an olivine fractionation correction using the East Greenland Lower Basalts data by assuming residual olivine of Fo_{88-91} , resulting in higher MgO (15.2–19.7 wt%) and lower SiO_2 (48.2–47.2 wt%). As emphasized in Section 1, their method depends on the assumption of a primary liquid Mg#, which now seems questionable, especially for lavas near ‘hotspots’. Correction for fractional crystallization to a liquid in equilibrium with Fo_{90} olivine yields a Ni-rich liquid, with 4400–5500 ppm Ni in coexisting olivine.

Icelandic data [11,31,34,35] show a distinct difference in FeO between Theistareykir (North Iceland) and the rest of the neovolcanic zones, among which only the western rift zone (Southwest Iceland) has sufficient data for our study. As already noted, liquid FeO varies little during olivine-only fractionation, so that the FeO content of high-MgO lava is a good proxy for its primary FeO content [5]. These two segments in Iceland, therefore, are considered separately in the fractionation correction (Fig. 4c,d).

In general, primary melt from the western rift zone is similar to that of Southeast Greenland, and lower in SiO_2 and higher in FeO and TiO_2 compared to that of Theistareykir. Equilibrium olivine for the western rift zone has lower Fo (~ 0.878) than Theistareykir (~ 0.900). This contrast in the Fo content in Icelandic lavas is maintained even with a multiphase fractionation correction, and continues to adjacent segments of the Mid-Atlantic Ridge. The Kolbeinsey Ridge data are almost indistinguishable from the Theistareykir data (Fig. 4d), whereas the Reykjanes Ridge data are akin to the western rift zone, and distinct from the Kolbeinsey Ridge (Fig. 4c). Due to limited data, however, this inference is preliminary.

Finally, ‘normal’ mid-ocean ridges far from hotspots are considered to provide a reference.

Table 1

Estimated primary melt compositions for the North Atlantic igneous province and normal mid-ocean ridges

Location	N ^a	SiO ₂	TiO ₂	Al ₂ O ₃	Fe ₂ O ₃	FeO	MnO	MgO	CaO	Na ₂ O	K ₂ O	Ni	
A. Average composition of high-MgO aphyric lavas													
E Greenland	8	49.1	1.96	13.8	0.6	10.8	0.31	9.4	12.1	1.81	0.21	204	
SE Greenland	11	48.1	1.42	15.3	0.6	10.9	0.21	10.5	10.3	2.34	0.20	223	
SW Iceland	5	47.5	1.71	15.2	0.7	11.6	0.20	9.3	11.4	2.07	0.21	149	
Theistareykir	69	48.7	0.98	15.3	0.6	9.6	0.18	10.3	12.5	1.82	0.10	189	
Reykjanes Ridge	2	50.1	1.03	14.4	0.6	10.3	0.18	9.2	11.8	2.19	0.07	167	
Kobeinsey Ridge	2	49.2	0.85	15.5	0.5	8.8	0.17	9.6	13.6	1.74	0.03	157	
MAR 22°–46°N	6	49.6	1.19	16.1	0.5	8.9	0.16	9.3	11.5	2.62	0.14	174	
EPR 2°–23°N	65	49.8	1.23	16.4	0.5	8.5	0.16	8.9	11.8	2.60	0.09	134	
Indian 43°–138°E	7	50.3	1.27	16.6	0.5	7.8	0.18	9.1	11.0	3.11	0.15	162	
Location	N	SiO ₂	TiO ₂	Al ₂ O ₃	Fe ₂ O ₃	FeO	MnO	MgO	CaO	Na ₂ O	K ₂ O	Fo ^b	V _p ^c
B. Multiphase fractionation correction with maximum Ni content of 3500 ppm													
E Greenland	8	48.6	1.68	14.4	0.6	10.1	0.18	10.9	11.5	1.83	0.18	0.865	7.11
SE Greenland	11	47.4	1.25	14.3	0.6	10.7	0.18	13.7	9.4	2.15	0.18	0.882	7.14
SW Iceland	5	46.9	1.38	14.7	0.6	10.9	0.16	12.9	10.3	1.93	0.17	0.875	7.16
Theistareykir	69	47.8	0.82	14.3	0.5	9.3	0.15	14.0	11.2	1.68	0.09	0.898	7.22
Reykjanes Ridge	2	49.3	0.85	14.6	0.6	9.7	0.15	11.8	11.0	2.10	0.06	0.879	7.12
Kobeinsey Ridge	2	48.2	0.68	15.0	0.5	8.2	0.14	13.2	12.3	1.65	0.02	0.905	7.22
MAR 22°–46°N	6	49.0	0.99	16.0	0.5	8.4	0.13	11.6	10.8	2.46	0.12	0.891	7.09
EPR 2°–23°N	65	48.8	0.97	16.2	0.5	7.8	0.12	12.4	10.8	2.40	0.07	0.902	7.12
Indian 43°–138°E	7	49.5	1.06	16.6	0.4	7.3	0.15	11.4	10.4	2.90	0.13	0.903	7.04
C. Olivine fractionation correction with maximum Ni content of 3500 ppm													
E Greenland	8	48.4	1.81	12.8	0.6	11.0	0.19	12.1	11.2	1.68	0.30	0.867	7.13
SE Greenland	11	47.4	1.28	13.8	0.6	11.0	0.19	14.1	9.3	2.11	0.18	0.883	7.15
SW Iceland	5	46.5	1.48	13.1	0.7	11.8	0.17	14.4	9.8	1.79	0.18	0.878	7.19
Theistareykir	69	47.7	0.86	13.5	0.6	9.7	0.16	14.8	11.0	1.60	0.09	0.900	7.24
Reykjanes Ridge	2	49.1	0.92	12.9	0.6	10.5	0.16	13.2	10.6	1.96	0.06	0.881	7.15
Kobeinsey Ridge	2	48.0	0.73	13.6	0.5	9.0	0.15	14.6	11.9	1.51	0.03	0.907	7.26
MAR 22°–46°N	6	48.8	1.07	14.6	0.5	9.1	0.14	12.9	10.5	2.36	0.13	0.893	7.12
EPR 2°–23°N	65	48.5	1.07	14.2	0.5	8.7	0.14	14.3	10.2	2.25	0.08	0.906	7.16
Indian 43°–138°E	7	49.3	1.15	15.1	0.5	8.0	0.16	12.8	10.0	2.82	0.14	0.905	7.07
Location	N	SiO ₂	TiO ₂	Al ₂ O ₃	Fe ₂ O ₃	FeO	MnO	MgO	CaO	Na ₂ O	K ₂ O	Ni(ol)	V _p
D. Olivine fractionation correction with maximum forsterite content of 0.90													
E Greenland	8	47.4	1.58	11.2	0.6	10.9	0.17	16.6	9.8	1.47	0.17	5524	7.25
SE Greenland	11	46.8	1.18	12.8	0.6	11.0	0.17	16.6	8.6	1.96	0.17	4413	7.21
SW Iceland	5	45.9	1.33	11.9	0.7	11.6	0.15	17.7	8.9	1.62	0.17	4564	7.28
Theistareykir	69	47.7	0.85	13.5	0.6	9.7	0.16	14.7	11.1	1.60	0.09	3392	7.24
Reykjanes Ridge	2	48.4	0.85	11.9	0.6	10.5	0.15	15.9	9.7	1.81	0.06	4489	7.22
Kobeinsey Ridge	2	48.2	0.74	14.0	0.5	8.9	0.15	13.5	12.3	1.55	0.03	2946	7.24
MAR 22°–46°N	6	48.5	1.05	14.2	0.5	9.1	0.14	13.8	10.2	2.31	0.12	3754	7.14
EPR 2°–23°N	65	48.7	1.09	14.6	0.5	8.7	0.14	13.2	10.6	2.31	0.08	3068	7.13
Indian 43°–138°E	7	49.5	1.16	15.4	0.5	8.0	0.17	12.1	10.2	2.88	0.14	3083	7.05

Values for oxide concentration are in wt%. The oxides have been normalized to a total of 100, and Fe³⁺/ΣFe of 0.05 is assumed. Ni concentrations are in ppm.

^aNumber of data.

^bFo content of equilibrium olivine based on $K_D = 0.30$.

^cTheoretical compressional-wave velocity of solidified phase at 600 MPa and 400°C. Values are in km/s. (see [37] for the details of calculation).

Analyses of glass samples from the East Pacific Rise (EPR) from 2°N to 23°N, the Indian Ocean from 43°E to 138°E, and the Mid-Atlantic Ridge from 22°N to 46°N, were downloaded from the RIDGE Petrological Database at Lamont Doherty Earth Observatory. The main sources for these data include [39–43]. The results of fractionation correction are shown in Fig. 4e. These samples, together with the Kolbeinsey Ridge data, extend over most of the ‘global trend’ of mid-ocean ridge basalt composition [5]. The primary melt for the EPR has higher FeO and lower Na₂O than that for the Indian Ocean, consistent with the global trend of Na_{8.0} and Fe_{8.0} [5,6]. Fo in equilibrium olivine is 0.902–0.906 for both regions, while the primary melt for the North Atlantic has lower Fo (0.891).

Regional averages of estimated primary melt composition are summarized in Table 1. An estimate based on correction to equilibrium olivine with Fo of 0.90 is also shown. This Fo-based correction results in very high Ni concentration (>4000 ppm) in equilibrium olivine for East Greenland, Southeast Greenland, Southwest Iceland and the Reykjanes Ridge. Thus, either the entire region is underlain by mantle with anomalously high Ni, or the amount of olivine addition required by the Fo₉₀ criterion is too high for this area. The liquids derived using a Ni criterion are very different in MgO and Mg# from those yielded using an Fo₉₀ criterion, while the differences in FeO, TiO₂ and Na₂O are minor. Estimated melts using the Fo₉₀ criterion range up to ~18 wt% MgO (25 mol%), implying mantle temperatures of ~1400°C [18]

The MgO and FeO contents of estimated primary melts based on the Ni criterion are plotted in Fig. 5, together with those of mantle melts from recent experimental studies at a range of

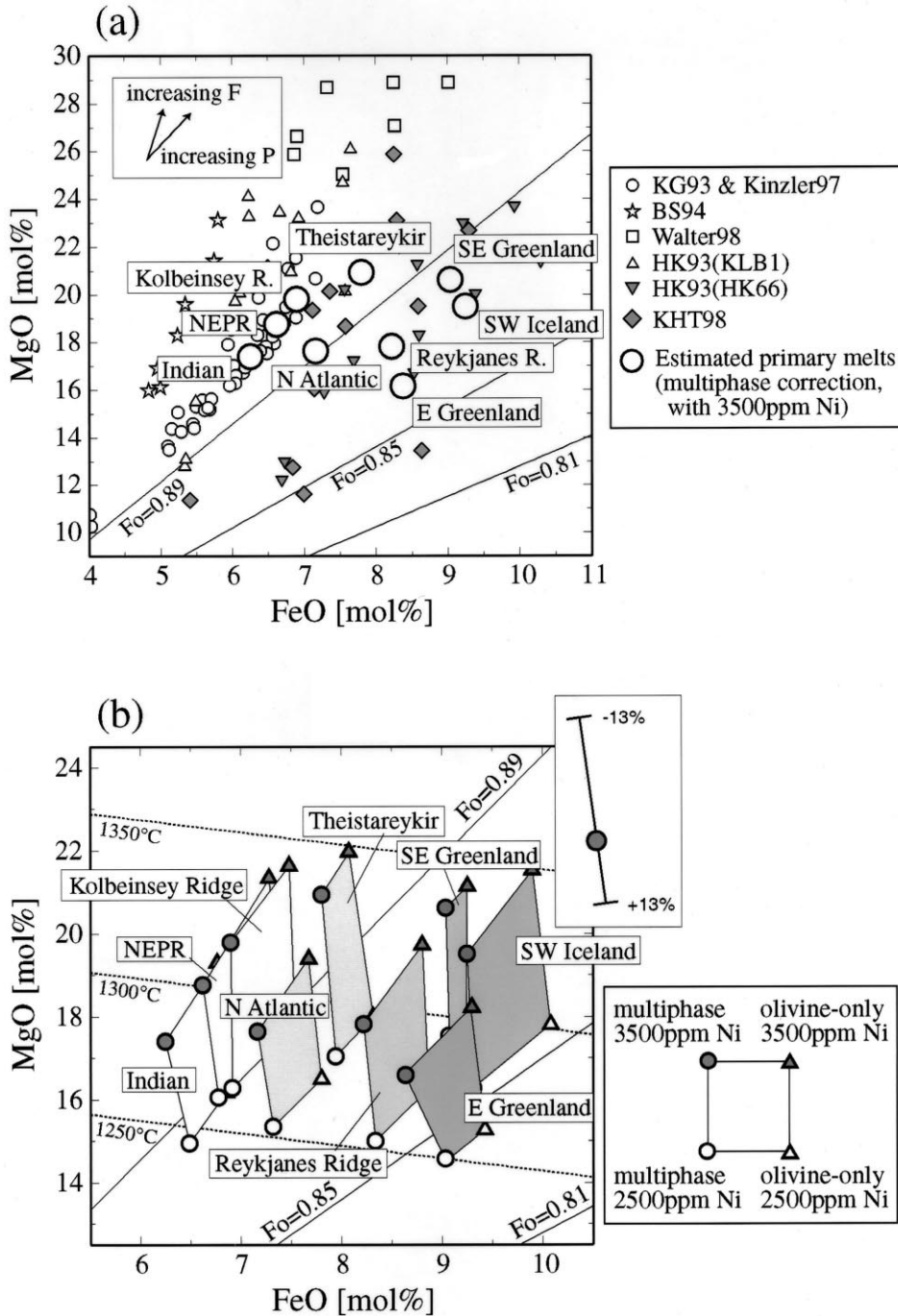
mantle pressures [7,27,28,44–47]. Most of these studies used mantle peridotites with whole rock Mg#s of 0.89–0.90. Exceptions are the pyroxenite HK66 used by Hirose and Kushiro [45] (whole rock Mg# of 0.854), and two homogeneous mixtures of peridotite and basalt, KG1 and KG2, used by Kogiso et al. [47] (whole rock Mg#s of 0.811 and 0.848, respectively). The composition of incipient melt is in equilibrium with the forsterite content of the source olivine, or approximately with whole rock Mg#. As melting proceeds, the liquid Mg# increases due to source depletion, regardless of the style of melting (e.g. batch and fractional), so that the Mg# of primary melt can be used to determine the Mg# of residual olivine, and to place an upper bound on the Fo content of source olivine.

Fig. 5a indicates that, whereas source mantle for North Iceland (Theistareykir) and the Kolbeinsey Ridge, as well as the Northern EPR and the Indian Ocean probably has compositions similar to ‘pyrolite’ (i.e. whole rock Mg# of ~0.895) (e.g. [48]), other regions in the North Atlantic igneous province must have source mantle with Mg#s lower than 0.87–0.88. Such a composition could result from 20–30% addition of basalt to mantle pyrolite. Table 1 shows that FeO contents > 10 wt% (~9 mol% FeO in Fig. 5a) are characteristic of primary melts estimated using both the Ni in olivine and Fo₉₀ criteria for SW Iceland, the Reykjanes Ridge, and the two Greenland sites. In contrast, all other areas we considered have estimated FeO < 10 wt%. Melts with > 10 wt% FeO have not been produced in experiments on mantle peridotites with compositions similar to pyrolite at pressures less than 4 GPa [28]. Alternatively, melting of more Fe-rich peridotite compositions can produce melts with Fe > 10 wt% at much lower pressure.

Fig. 5. (a) Molar FeO and MgO contents of estimated primary melts based on the 3500 ppm olivine Ni criterion with multiphase fractionation correction are plotted with those of experimental mantle melts from [7,27,28,44–47]. Fe³⁺/ΣFe of 0.05 is assumed. The Fo content of equilibrium olivine is shown as thin lines, assuming $K_d^{Fe/Mg} = 0.30$. (b) Molar FeO and MgO contents of estimated primary melts based on the 2500–3500 ppm olivine Ni criterion are plotted for both multiphase and olivine-only fractionation corrections. Liquid temperature based on the olivine-liquid thermometer of Roeder and Emslie [18] is indicated by the dashed line. The errors in the MgO and FeO contents owing to the prediction error of $D_{Ni}^{ol/liq}$ (one S.D. of ±13% [21]) are also shown. Roughly speaking, the one S.D. range of $D_{Ni}^{ol/liq}$ is equivalent to varying maximum Ni content from 500 ppm lower to 1000 ppm higher.

Fig. 5b illustrates the estimated uncertainty in our calculated primary melts. We show results from olivine-only and olivine+plagioclase back-fractionation, and using endpoints at olivine Ni

contents of 2500 and 3500 ppm. An inset shows the uncertainty in Mg and Fe contents of primary melts introduced by uncertainty in $D_{Ni}^{ol/liq}$ [21]. If all uncertainties illustrated here are combined, or



if the maximum values for Mg content are close to the true values for some areas and are much higher than the true values elsewhere, then there could be no heterogeneity in source Mg# in the North Atlantic igneous province. However, note that this would require systematic variation in source Ni content, fractionating phase proportions, and/or $D_{\text{Ni}}^{\text{ol/liq}}$ with geographical area. In the absence of evidence to the contrary, we think such systematics are unlikely.

Another interesting observation regarding Fig. 5 is that the temperature of the primary melts does not vary significantly between the North Atlantic igneous province and normal mid-ocean ridges. The temperature difference between EPR and SW Iceland, for example, is about 20°C if compared at the same olivine Ni content, and is only about 70°C even if there is a 1000-ppm difference in the Ni content of equilibrium olivine. We used the olivine–liquid thermometer of Roeder and Emslie [18] for Fig. 5b, but the more recent thermometer of Gaetani and Grove [49] predicts similarly small temperature variation.

One way to raise the estimated temperature of Iceland and Greenland primary melts as high as expected from thermal plume hypotheses seems to be to assume that the mantle beneath these areas has a higher oxygen fugacity, which effectively reduces the amount of olivine addition required during fractionation correction and increases the Mg# of estimated primary melt. Fig. 6 shows the sensitivity of our fractionation correction to the oxidation state of primary melt. $\text{Fe}^{3+}/\Sigma\text{Fe}$ greater than 0.20 is required to increase the Fo content of residual olivine in equilibrium with Iceland and Greenland primary melts to 0.90. This appears unrealistic on the basis of our understanding of the mantle oxidation state (e.g. [36,50]).

Alternatively, as mentioned above, Iceland and Greenland mantle residues could have a ‘normal’ Mg# combined with anomalously high Ni and very high temperature. This also appears unlikely in view of the nearly complete lack of high-Ni compositions among mantle peridotite samples. In any case, if the mantle source for SW Iceland and Greenland primary melts were far more oxidized or Ni-rich than the source for, e.g., Theis-

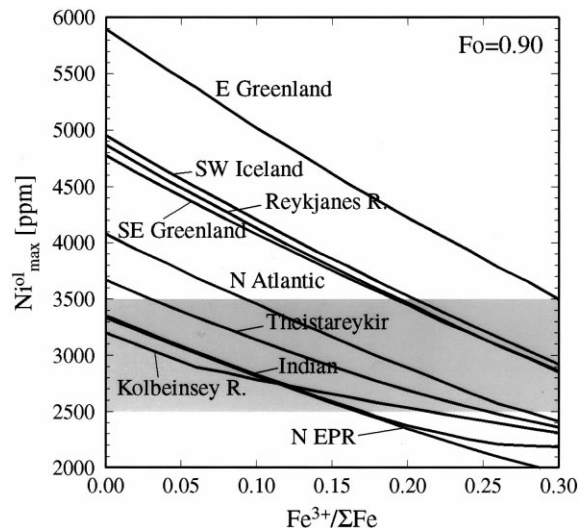


Fig. 6. The Ni content of equilibrium olivine for primary melts estimated on the basis of the criterion of $\text{Fo}=0.90$ is plotted as a function of $\text{Fe}^{3+}/\Sigma\text{Fe}$.

tareykir and MORB, this would also constitute a dramatic major element heterogeneity.

4. Possible open-system effects

The Ni criterion is useful to discriminate high-MgO samples with an olivine cumulative origin or which have been modified by olivine dissolution. The most primitive lavas, i.e., aphyric lavas with the highest MgO content, can place a lower bound on the primary MgO content. Ideally, however, this inference should be supported by Ni concentration, because petrographic criteria may be misleading [20,21,51]. Fig. 4a,b show that misinterpretation of picritic samples can be avoided in some cases by calculating the Ni content of equilibrium olivine.

Dissolution of olivine could occur where adiabatically ascending melt reacts with high temperature olivine in the upper mantle or lower crust. A rough estimate of the maximum possible amount of olivine dissolution can be obtained by considering energy balance. Because the melt adiabat is ~ 10 K/GPa and the pressure dependency of the olivine saturation temperature is ~ 50 – 100 K/GPa in the lower crust or upper mantle, adiabati-

cally ascending liquid can be ‘superheated’ by 40–90 K/GPa. If the temperature of ‘wall rock’ olivine is close to the liquidus temperature, liquid that is 40 K above its olivine saturation temperature can dissolve as much as 7 wt% olivine relative to the original liquid mass, given a specific heat of $1 \text{ kJ kg}^{-1} \text{ K}^{-1}$ and a latent heat of fusion of 600 kJ kg^{-1} [52]. This substantially modifies liquid Mg and Ni contents, as shown in Fig. 7.

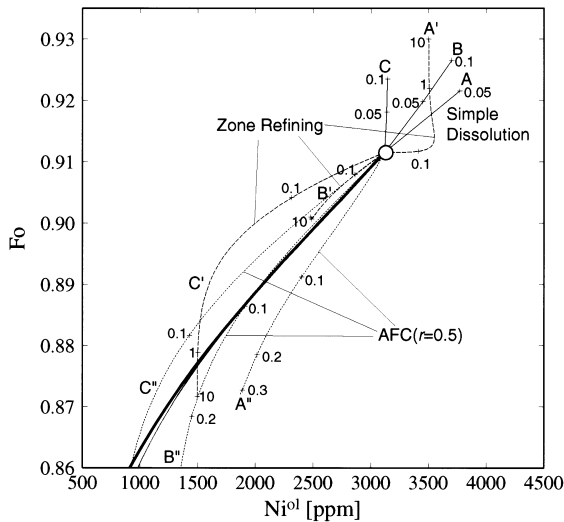


Fig. 7. An example of assimilation and fractional crystallization modeling with the starting liquid B in Fig. 3 (shown as open circle). The starting liquid is assumed to be in equilibrium with olivine with 3000 ppm Ni. Three olivine compositions are chosen as assimilant: A (Fo_{93} , 3500 ppm Ni), Fo_{90} , 2480 ppm Ni), and C (Fo_{87} , 1500 ppm Ni). An olivine-only fractionation model is used to prepare olivine compositions B and C with consistent Fo and Ni contents. We model (1) simple dissolution (AFC with $r = \infty$, thin solid lines A, B, and C with 5% tick interval for assimilant mass), (2) zone refining (AFC with $r = 1.0$, dashed lines A', B', and C'), (3) AFC with $r = 0.5$ (dotted lines A'', B'', and C''), (4) simple fractional crystallization (AFC with $r = 0$, thick solid line), and (5) periodically replenished magma chamber with constant mass (gray line). The parameter r is defined as \dot{M}_a/\dot{M}_c , where \dot{M}_a and \dot{M}_c are the mass assimilated and the mass crystallized, respectively [56]. Ticks are shown for the amount of dissolved olivine with respect to the original liquid mass. Only liquids with 8 to 18 wt% MgO are shown in this diagram. The model results are shown in terms of the Ni and Fo contents of equilibrium olivine. By comparing with the liquid line of descent defined by simple fractional crystallization, one can see how open-system evolution affects the estimate of the Mg# of residual mantle olivine using our Ni-based fractionation correction. See text for discussion.

Small amounts of olivine dissolution, if undetected, would lead to an overestimate of primary melt Mg#.

The most forsteritic olivine phenocrysts are also commonly used to estimate primary liquid MgO content [51,53]. Mantle melts are generally considered to be the aggregate of polybaric partial melts with different Mg#s. What we attempt to estimate in this study is the *mean* Mg# of aggregate primary melt and thus the mean Fo content of residual olivine. On the other hand, using the most forsteritic olivine crystals observed in lavas can be biased to the most depleted, shallowest end member. Regarding continental flood basalts, there is an additional caveat. Southeast Greenland samples, for example, include large, euhedral olivine phenocrysts with $\text{Fo}_{90.2-92.4}$ [54]. Thy et al. [30] inferred that the high-MgO lavas ($\sim 18 \text{ wt}\%$ MgO) with such high-Fo olivines are a possible primary melt. Instead, however, such high-Fo olivine may indicate the interaction of magma with depleted continental mantle at a low melt/rock ratio. Indeed, mantle xenoliths from the cratonic lithosphere have highly forsteritic olivines (e.g. mean of $\text{Fo}_{92.7}$ for East Greenland samples) [55] (Fig. 2e). Interaction with depleted continental lithosphere can, therefore, introduce significant ambiguity in determining primary melt composition, especially for continental flood basalts. We recommend testing for such interaction by calculating equilibrium olivine Ni contents, and then rejecting samples in equilibrium with olivine having more than 3500 ppm Ni.

In addition to olivine dissolution, there are a variety of open-system processes which might produce apparent heterogeneity in the Mg# of the North Atlantic mantle source. Because compatibility with olivine increases in the order of Fe, Mg and Ni, reaction with olivine in the upper mantle or lower crust may significantly decouple liquid Ni from Mg#, compared to the trend for fractional crystallization. In some cases, the fractionation correction based on the Ni content could underestimate primary liquid Mg#. To explore this possibility, we conducted assimilation and fractional crystallization (AFC) modeling [56,57] with a range of input parameters. The results would be similar for continuous replenishment

of a magma chamber undergoing fractionation. Representative results, for liquid MgO contents between 8 and 18 wt%, are shown in Fig. 7. To lower equilibrium olivine Mg# by 0.01 at high Ni the olivine reactant has to have a high Fo content (>0.90), and the amount of reacted olivine has to be large relative to the original liquid mass. This kind of open-system evolution might potentially lead to an underestimate of primary melt Mg# using our olivine fractionation correction. However, Fig. 5 shows that the potential errors introduced by overlooking open-system effects would have to be systematically related to location within the North Atlantic igneous province. In the absence of evidence to the contrary, we believe that such a systematic relationship is unlikely.

5. Discussion and conclusion

Our case study shows that olivine fractionation correction with the Ni criterion is a promising approach to estimate the composition of primary melt. Though the number of data appropriate for our scheme is small, this method is especially useful to constrain the extent of Mg# source heterogeneity. Because the major element composition of mantle-derived melt is very sensitive to both source composition and melting process, the interpretation of lava chemistry solely on the basis of compositional systematics is often equivocal. The high FeO content of the Southwest Iceland lavas, for example, has been known for decades (e.g. [10,58]), but it has been attributed only to the melting process or previous depletion history, based on a correlation with La/Sm ratio. Fram and Leshner [9] estimated primary melts for various regions of the North Atlantic igneous province using olivine fractionation with a predetermined liquid Mg# and, based on a correlation with Dy/Yb ratio, concluded that the East Greenland Tertiary flood basalts resulted from the melting of Fe-poor mantle, at odds with our result. On the other hand, Scarrow and Cox [59] proposed Fe-rich source mantle for the Skye Main Lava Series in Northwest Scotland, but their work is based on the whole rock composition of

polyphyric lavas, which contain up to 20% olivine phenocrysts of Fo_{80–86}.

Up to this point, we have concentrated on evidence for possible heterogeneity in mantle Mg# and/or oxygen fugacity in the North Atlantic. However, the processes that might produce such heterogeneity, for example, via addition of subducted metabasalt to the convecting mantle, are likely to give rise to substantial trace element variation as well. Thus, the inferred variation in source Mg# is expected to be correlated with trace element variation. Unfortunately, it is difficult to separate the effects of melting processes from those of source composition using trace element contents of lavas. It is potentially easier to

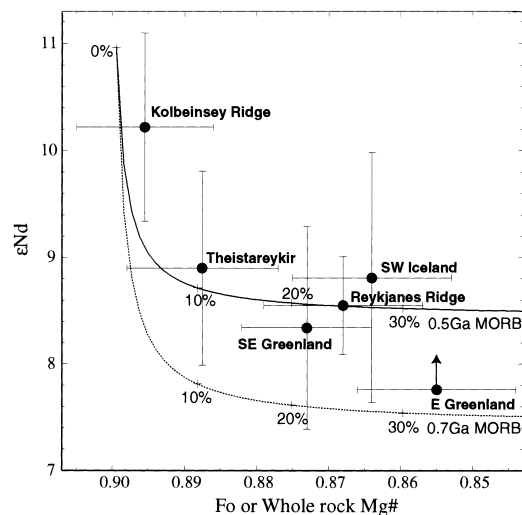


Fig. 8. The covariation of ϵNd and estimated maximum Fo content of residual mantle olivine for the six regions in the North Atlantic igneous province. Nd isotope data are compiled from the literature. Whereas error bars for ϵNd denote one S.D. of sample statistics, those for the Fo content denote the ambiguity of mean estimated value corresponding to maximum olivine Ni contents ranging from 2500–3500ppm. The effect of continental crustal contamination on East Greenland samples is significant, so we take the highest ϵNd value from available data. To illustrate the effect of basalt addition, mixing curves between depleted pyrolite mantle and 0.5 Ga (solid) or 0.7 Ga (dashed), normal MORB are also shown. See text for the details of the mixing calculation. The mixing calculation provides the Mg# of source mantle, which is \leq the Mg# of residual mantle. Correction for the effect of melting on Mg# would shift all data points to the left, possibly by variable amounts, but probably would not change the overall systematics.

detect ‘long-lived’ trace element heterogeneity using radiogenic isotope ratios. Sr isotopes are potentially affected by alteration, particularly in the older samples of East Greenland, while Pb- and Hf-isotope data are rare for the Tertiary lavas. Thus, we have compiled Nd-isotope data for the North Atlantic localities where Mg# heterogeneity is proposed to be present.

In Fig. 8, we show predicted Mg# in olivine equilibrated with primary melt versus average ϵ_{Nd} for each area. These data, while not conclusive, are permissive of long-lived mantle heterogeneity in which source Mg# is correlated with Sm/Nd. As mentioned above, we think that the simplest explanation for substantial variation of Mg# in the convecting mantle is mixing between subducted basalt and an otherwise homogeneous MORB source. For illustrative purposes, we show the effect of mixing basalt with depleted mantle. The $^{143}\text{Nd}/^{144}\text{Nd}$ and $^{147}\text{Sm}/^{144}\text{Nd}$ of depleted mantle are estimated to be 0.5132 and 0.239, respectively, using $^{143}\text{Nd}/^{144}\text{Nd}$ of Atlantic MORB and the Bulk Earth 2-Ga geochron to derive $^{147}\text{Sm}/^{144}\text{Nd}$ [60]. Major element and Nd concentrations are from [44] and [61]. The isotopic ratios of recycled, normal MORB are estimated by assuming that it was derived from depleted mantle sometime in the past with the same Sm/Nd fractionation as inferred for present-day Atlantic MORB. The major element and Nd concentrations of normal MORB are taken from Hofmann [62]. Note that this method assumes that pyrolite and MORB isotopic reservoirs remained isolated and did not mix until shortly prior to melting.

Fig. 8 suggests that the covariation of the Nd isotope data and the estimated Fo contents of residual mantle olivine could be explained by mixing depleted pyrolite mantle and recycled, normal MORB generated at about 0.6 Ga. Mixing pyrolite with older MORB cannot explain the small ϵ_{Nd} variation observed in the North Atlantic igneous province. We were initially tempted to correlate the ‘age’ of the basaltic component in Fig. 8 with the time of subduction along the Caledonian suture zone, which lies close to the East Greenland margin. However, this could be misleading. Our example of a mixing calculation is

insufficient to capture all details of North Atlantic mantle heterogeneity (e.g. [63,64]). Recent work on mantle geochemistry suggests mixing of depleted continental mantle, subducted sediment, altered upper oceanic crust, lower oceanic crust and delaminated lower continental crust, as well as ingrowth of ^{143}Nd in mixed compositions. An additional, intriguing possibility is that interaction at the core–mantle boundary formed a high-Ni mantle source. However, such complicated models for the North Atlantic province seem premature due to the abundance of variables combined with the paucity of data.

Crustal thickness and seismic velocity have been used to infer the potential temperature and dynamics of mantle upwelling during continental rifting (e.g. [65,66]). Bulk or lower crustal velocity can be used as a proxy for primary melt composition, which in turn can be used to constrain the average pressure and fraction of mantle melting, and thus the mantle potential temperature. Such an estimate can be compared to the observed volume of igneous crust. Where crustal thickness is too large to be explained by passive mantle upwelling at the potential temperature inferred from seismic velocity, then one may call upon ‘active’ mantle convection during rifting. Obviously, this procedure is critically dependent on the method used to infer primary melt composition from seismic data. Korenaga et al. [67] used partial melts of mantle compositions similar to pyrolite to generate a function relating the two. Our study was initiated to check this procedure. In fact, the assumption of a pyrolite source composition for thick igneous crust along rifted margins is open to question.

In Table 1, theoretical compressional-wave velocity at 600 MPa and 400°C is reported for each primary melt composition. The bulk crustal velocity of 30-km-thick igneous crust at the Southeast Greenland margin is observed to be lower than ~ 7.0 km/s [66]. The Southeast Greenland primary melt based on the 3500 ppm Ni criterion has a velocity > 7.1 km/s, exceeding the seismic estimate. Because seismic velocity is most sensitive to MgO content, this discrepancy may result from our upper bound approach, so that the true primary melt may have even lower MgO, increasing

the inferred extent of major element source heterogeneity. If the Greenland margin was indeed underlain by low Mg# mantle during rifting, this could help to explain the combination of relatively low seismic velocity with thick igneous crust. All other things being equal, low Mg# peridotite is expected to be more 'fertile' than pyrolyte, producing more melt, with lower MgO, at a given mantle potential temperature.

In summary, though our understanding of the spatial extent of source heterogeneity is still at a preliminary stage due to the limited amount of suitable data, this study suggests that long-standing, major element heterogeneity had an important role in the formation of thick igneous crust in the North Atlantic province. This heterogeneity must include regionally extensive, anomalously low Mg#, and/or high oxygen fugacity, and/or high Ni contents, in the mantle source for SW Iceland, Reykjanes Ridge and East Greenland primary melts. Low Mg# is the most likely variable. Such heterogeneity could have arisen via a multitude of possible processes, among which we emphasize mixing of depleted mantle with recycled oceanic crust. It is important to account for such heterogeneity, and its effect on productivity during mantle melting, when inferring the conditions of mantle melting from lava compositions and/or seismic data.

Acknowledgements

This paper has benefitted from discussions with Nobu Shimizu, Ken Koga, Greg Hirth, Tim Grove, Steve Parman, Kirsten Nicolaysen, Jim Van Orman, Karen Hanghøj and Chip Lesher. We thank Pam Kempton and Barry Hanan for sending us preprints of their work, and Janne Blichert-Toft for additional advice on North Atlantic isotope values. Lotte Larsen, Barry Hanan, Francis Albarede, and an anonymous reviewer provided careful and constructive reviews. This work was supported by NSF grant OCE-9416631. [FA]

References

- [1] J.C. Mutter, C.M. Zehnder, Deep crustal structure and magmatic processes: the inception of seafloor spreading in the Norwegian-Greenland Sea, in: A.C. Morton, L.M. Parson (Eds.), *Early Tertiary Volcanism and the Opening of the NE Atlantic*, Geol. Soc. Spec. Publ. 39, 1988, pp. 35–48.
- [2] H.C. Larsen, S. Jakobsdóttir, Distribution, crustal properties and significance of seawards-dipping sub-basement reflectors off E Greenland, in: A.C. Morton, L.M. Parson (Eds.), *Early Tertiary Volcanism and the Opening of the NE Atlantic*, Geol. Soc. Spec. Publ. 39, 1988, pp. 95–114.
- [3] R. White, D. McKenzie, Magmatism at rift zones: the generation of volcanic continental margins and flood basalts, *J. Geophys. Res.* 94 (1989) 7685–7729.
- [4] M.A. Richards, R.A. Duncan, V.E. Courtillot, Flood basalts and hot-spot tracks: plume heads and tails, *Science* 246 (1989) 103–107.
- [5] E.M. Klein, C.H. Langmuir, Global correlations of ocean ridge basalt chemistry with axial depth and crustal thickness, *J. Geophys. Res.* 92 (1987) 8089–8115.
- [6] C.H. Langmuir, E.M. Klein, T. Plank, Petrological systematics of mid-ocean ridge basalts: constraints on melt generation beneath ocean ridges, in: J. Phipps Morgan, D.K. Blackman, J.M. Sinton (Eds.), *Mantle Flow and Melt Generation at Mid-Ocean Ridges*, Geophys. Monogr. Ser. 71, AGU, Washington, DC, 1992, pp. 183–280.
- [7] R.J. Kinzler, T.L. Grove, Primary magmas of mid-ocean ridge basalts. 2: Applications, *J. Geophys. Res.* 97 (1992) 6907–6926.
- [8] T.L. Grove, R.J. Kinzler, W.B. Bryan, Fractionation of mid-ocean ridge basalt (MORB), in: *Mantle Flow and Melt Generation at Mid-Ocean Ridges*, American Geophysical Union, 1992, pp. 281–310.
- [9] M.S. Fram, C.E. Lesher, Generation and polybaric differentiation of East Greenland Early Tertiary flood basalts, *J. Petrol.* 38 (1997) 231–275.
- [10] C.H. Langmuir, G.N. Hanson, An evaluation of major element heterogeneity in the mantle sources of basalts, *Phil. Trans. R. Soc. Lond. A* 297 (1980) 383–407.
- [11] J.-G. Schilling, M. Zajac, R. Evans, T. Johnson, W. White, J.D. Devine, R. Kingsley, Petrologic and geochemical variations along the Mid-Atlantic Ridge from 29°N to 73°N, *Am. J. Sci.* 283 (1983) 510–586.
- [12] E.H. Hauri, Major-element variability in the Hawaiian mantle plume, *Nature* 382 (1996) 415–419.
- [13] E. Takahashi, K. Nakajima, T.L. Wright, Origin of the Columbia River basalts: melting model of a heterogeneous plume head, *Earth Planet. Sci. Lett.* 162 (1998) 63–80.
- [14] F.A. Frey, C.-Y. Suen, H.W. Stockman, The Ronda high temperature peridotite: geochemistry and petrogenesis, *Geochim. Cosmochim. Acta* 49 (1985) 2469–2491.
- [15] C.J. Allègre, D.L. Turcotte, Implications of a 2-component marble-cake mantle, *Nature* 323 (1986) 123–127.

- [16] C.J. Allègre, M. Treuil, J.-F. Minster, B. Minster, F. Albarède, Systematic use of trace element in igneous process. I. Fractional crystallization processes in volcanic suites, *Contrib. Miner. Petrol.* 60 (1977) 57–75.
- [17] P.B. Kelemen, S.R. Hart, S. Bernstein, Silica enrichment in the continental upper mantle via melt/rock reaction, *Earth Planet. Sci. Lett.* 164 (1998) 387–406.
- [18] P.L. Roeder, R.F. Emslie, Olivine–liquid equilibrium, *Contrib. Miner. Petrol.* 29 (1970) 275–289.
- [19] P. Ulmer, The dependence of the Fe²⁺-Mg cation-partitioning between olivine and basaltic liquid on pressure, temperature and composition: an experimental study to 30 kbars, *Contrib. Miner. Petrol.* 101 (1989) 261–273.
- [20] S.R. Hart, K.E. Davis, Nickel partitioning between olivine and silicate melt, *Earth Planet. Sci. Lett.* 40 (1978) 203–219.
- [21] R.J. Kinzler, T.L. Grove, S.I. Recca, An experimental study on the effect of temperature and melt composition on the partitioning of nickel between olivine and silicate melt, *Geochim. Cosmochim. Acta* 54 (1990) 1255–1265.
- [22] J.S. Weaver, C.H. Langmuir, Calculation of phase equilibrium in mineral-melt systems, *Comp. Geosci.* 16 (1990) 1–19.
- [23] H.-J. Yang, R.J. Kinzler, T.L. Grove, Experiments and models of anhydrous, basaltic olivine–plagioclase–augite saturated melts from 0.001 to 10 kbar, *Contrib. Miner. Petrol.* 124 (1996) 1–18.
- [24] J.L. Bodinier, C. Dupuy, J. Dostal, C. Merlet, Distribution of trace transition elements in olivine and pyroxenes from ultramafic xenoliths: application of microprobe analysis, *Am. Miner.* 72 (1987) 902–913.
- [25] C.H. Langmuir, Geochemical consequences of in situ crystallization, *Nature* 340 (1989) 199–205.
- [26] M.J. O'Hara, Geochemical evolution during fractional crystallisation of a periodically refilled magma chamber, *Nature* 266 (1977) 503–507.
- [27] M.B. Baker, E.M. Stolper, Determining the composition of high-pressure mantle melts using diamond aggregates, *Geochim. Cosmochim. Acta* 58 (1994) 2811–2827.
- [28] M.J. Walter, Melting of garnet peridotite and the origin of komatiite and depleted lithosphere, *J. Petrol.* 39 (1998) 29–60.
- [29] P.S. Meyer, H. Sigurdsson, J.-G. Schilling, Petrological and geochemical variations along Iceland's neovolcanic zones, *J. Geophys. Res.* 90 (1985) 10043–10072.
- [30] P. Thy, C.E. Leshner, M.S. Fram, Low pressure experimental constraints on the evolution of basaltic lavas from Site 917, Southeast Greenland continental margin, *Proc. Ocean Drill. Prog. Sci. Res.* 152 (1998) 359–372.
- [31] L. Slater, Melt Generation beneath Iceland, Ph.D. thesis, University of Cambridge, 1996.
- [32] L.M. Larsen, W.S. Watt, M. Watt, Geology and petrology of the lower Tertiary plateau basalts of the Scoresby Sund region, East Greenland, *Grøn. Geol. Unders. Bull.* 157 (1989) 1–162.
- [33] L.M. Larsen, J.G. Fitton, M.S. Fram, Volcanic rocks of the Southeast Greenland margin in comparison with other parts of the North Atlantic Tertiary igneous province, *Proc. Ocean Drill. Prog. Sci. Res.* 152 (1998) 315–330.
- [34] D.A. Wood, J.-L. Joron, M. Treuil, M. Norry, J. Tarney, Elemental and Sr isotope variations in basic lavas from Iceland and the surrounding ocean floor, *Contrib. Miner. Petrol.* 70 (1979) 319–339.
- [35] C.H. Hemond, N.T. Arndt, U. Lichtenstein, A.W. Hofmann, N. Oskersson, S. Steinthorsson, The heterogeneous Iceland plume: Nd–Sr–O isotopes and trace element constraints, *J. Geophys. Res.* 98 (1993) 15833–15850.
- [36] D.M. Christie, I.S.E. Carmichael, C.H. Langmuir, Oxidation states of mid-ocean ridge basalt glasses, *Earth Planet. Sci. Lett.* 79 (1986) 397–411.
- [37] J. Korenaga, Magmatism and Dynamics of Continental Breakup in the Presence of a Mantle Plume, Ph.D. thesis, MIT/WHOI Joint Program, 2000.
- [38] H.C. Larsen, A.D. Saunders, P.D. Clift, Shipboard Scientific Party, Proceedings of the Drilling Program Initial Report, vol. 152, Ocean Drill. Program, College Station, TX, 1994.
- [39] E.M. Klein, C.H. Langmuir, H. Staudigel, Geochemistry of basalts from the Southeast Indian Ridge, 115°E–138°E, *J. Geophys. Res.* 96 (1991) 2089–2107.
- [40] J.F. Bender, C.H. Langmuir, G.N. Hanson, Petrogenesis of basalt glasses from the Tamayo region, East Pacific Rise, *J. Petrol.* 25 (1984) 213–254.
- [41] Y. Niu, R. Batiza, Trace element evidence from seamounts for recycled oceanic crust in the eastern Pacific mantle, *Earth Planet. Sci. Lett.* 148 (1997) 471–483.
- [42] J.R. Reynolds, C.H. Langmuir, Petrological systematics of the Mid-Atlantic Ridge south of Kane: implications for ocean crust formations, *J. Geophys. Res.* 102 (1997) 14915–14946.
- [43] R. Hekinian, D. Walker, Diversity and spatial zonation of volcanic rocks from the East Pacific Rise near 21°N, *Contrib. Miner. Petrol.* 96 (1987) 265–280.
- [44] R.J. Kinzler, T.L. Grove, Corrections and further discussion of the primary magmas of mid-ocean ridge basalts, 1 and 2, *J. Geophys. Res.* 98 (1993) 22339–22347.
- [45] K. Hirose, I. Kushiro, Partial melting of dry peridotites at high pressures: Determination of compositions of melts segregated from peridotite using aggregates of diamond, *Earth Planet. Sci. Lett.* 114 (1993) 477–489.
- [46] R.J. Kinzler, Melting of mantle peridotite at pressures approaching the spinel to garnet transition: application to mid-ocean ridge basalt petrogenesis, *J. Geophys. Res.* 102 (1997) 852–874.
- [47] T. Kogiso, K. Hirose, E. Takahashi, Melting experiments on homogeneous mixtures of peridotite and basalt: application to the genesis of ocean island basalts, *Earth Planet. Sci. Lett.* 162 (1998) 45–61.
- [48] A.E. Ringwood, Compositions and Petrology of the Earth's Mantle, McGraw-Hill, New York, 1975.
- [49] G.A. Gaetani, T.L. Grove, The influence of water on melting of mantle peridotite, *Contrib. Miner. Petrol.* 131 (1998) 323–346.
- [50] B.J. Wood, L.T. Bryndzia, K.E. Johnson, Mantle oxida-

- tion state and its relationship to tectonic environment and fluid speciation, *Science* 248 (1990) 337–345.
- [51] D.B. Clarke, Tertiary basalts of Baffin Bay: possible primary magmas from the mantle, *Contrib. Miner. Petrol.* 25 (1970) 203–224.
- [52] M.J. Daines, D.L. Kohlstedt, The transition from porous to channelized flow due to melt/rock reaction during melt migration, *Geophys. Res. Lett.* 21 (1994) 145–148.
- [53] A.K. Pedersen, Reaction between picrite magma and continental crust early Tertiary silicic basalts and magnesian andesites from Disko, West Greenland, *Gronl. Geol. Unders. Bull.* 152 (1985) 1–126.
- [54] A. Demant, Mineral chemistry of volcanic sequences from Hole 917A, Southeast Greenland margin, *Proc. Ocean Drill. Prog. Sci. Res.* 152 (1998) 403–416.
- [55] S. Bernstein, P.B. Kelemen, C.K. Brooks, Highly depleted spinel harzburgite xenoliths in Tertiary dykes from East Greenland: restites from high degree melting, *Earth Planet. Sci. Lett.* 154 (1998) 221–235.
- [56] D.J. DePaolo, Trace element and isotopic effects of combined wallrock assimilation and fractional crystallization, *Earth Planet. Sci. Lett.* 53 (1981) 189–202.
- [57] P.B. Kelemen, Assimilation of ultramafic rock in subduction-related magmatic arcs, *J. Geol.* 94 (1986) 829–843.
- [58] S.P. Jakobsson, J. Jónsson, F. Shido, Petrology of the western Reykjanes Peninsula, Iceland, *J. Petrol.* 19 (1978) 669–705.
- [59] J.H. Scarrow, K.G. Cox, Basalts generated by decompressive adiabatic melting of a mantle plume: a case study from the Isle of Skye, NW Scotland, *J. Petrol.* 36 (1995) 3–22.
- [60] V.J.M. Salters, S.R. Hart, The hafnium paradox and the role of garnet in the source of mid-ocean-ridge basalts, *Nature* 342 (1989) 420–422.
- [61] S.-S. Sun, W.F. McDonough, Chemical and isotopic systematics of oceanic basalts: implications for mantle composition and processes, in: A.D. Saunders, M.J. Norry (Eds.), *Magmatism in the Ocean Basins*, Geological Society of London, 1989, pp. 313–345.
- [62] A.W. Hofmann, Chemical differentiation of the Earth: the relationship between mantle, continental crust and oceanic crust, *Earth Planet. Sci. Lett.* 90 (1988) 297–314.
- [63] B.B. Hanan, J. Blichert-Toft, R. Kingsley, J.-G. Schilling, Depleted Iceland mantle plume geochemical signature: artifact of multicomponent mixing?, *Geochem. Geophys. Geosys.* 1 (2000) 1999GC000009.
- [64] C. Chauvel, C. Hemond, Melting of a complete section of recycled oceanic crust: trace element and Pb isotopic evidence from Iceland, *Geochem. Geophys. Geosys.* 1 (2000) 1999GC000002.
- [65] P.B. Kelemen, W.S. Holbrook, Origin of thick, high-velocity igneous crust along the US East Coast Margin, *J. Geophys. Res.* 100 (1995) 10077–10094.
- [66] J. Korenaga, W.S. Holbrook, G.M. Kent, P.B. Kelemen, R.S. Detrick, H.C. Larsen, J.R. Hopper, T. Dahl-Jensen, Crustal structure of the Southeast Greenland margin from joint refraction and reflection seismic tomography, *J. Geophys. Res.* 105 (2000) 21591–21614.
- [67] J. Korenaga, P.B. Kelemen, W.S. Holbrook, Mantle melting and crustal accretion processes during continental breakups, with an example from the Southeast Greenland margin, *J. Geophys. Res.* (2000) submitted for publication.
- [68] F.R. Boyd, N.P. Pokhilenko, D.G. Pearson, S.A. Mertzman, N.V. Sobolev, L.W. Finger, Composition of the Siberian cratonic mantle: evidence from Udachnaya peridotite xenoliths, *Contrib. Miner. Petrol.* 128 (1997) 228–246.
- [69] W. McDonough, F. Frey, Rare earth elements of upper mantle rocks, in: B.R. Lipin, G.R. McKay (Eds.), *Geochemistry and Mineralogy of Rare Earth Elements*, *Rev. Mineral.* 21, Mineralogical Society of America, Washington, DC, 1989, pp. 99–145.
- [70] P.B. Kelemen, H.J.B. Dick, J.E. Quick, Formation of harzburgite by pervasive melt/rock reaction in the upper mantle, *Nature* 358 (1992) 635–641.